

A Unification Framework for Euclidean and Hyperbolic Graph Neural Networks

Mehrdad Khatir¹, Nurendra Choudhary¹, Sutanay Choudhury², Khushbu Agarwal², Chandan K. Reddy¹

¹Department of Computer Science, Virginia Tech, Arlington, VA, USA

²Pacific Northwest National Laboratory, Richland, WA, USA

{khatir, nurendra}@vt.edu, {sutanay.choudhury, khushbu.Agarwal}@pnnl.gov, reddy@cs.vt.edu

Abstract

Hyperbolic neural networks can effectively capture the inherent hierarchy of graph datasets, and consequently a powerful choice of GNNs. However, they entangle multiple incongruent (gyro-)vector spaces within a layer, which makes them limited in terms of generalization and scalability. In this work, we propose the Poincaré disk model as our search space, and apply all approximations on the disk (as if the disk is a tangent space derived from the origin), thus getting rid of all inter-space transformations. Such an approach enables us to propose a hyperbolic normalization layer and to further simplify the entire hyperbolic model to a Euclidean model cascaded with our hyperbolic normalization layer. We applied our proposed nonlinear hyperbolic normalization to the current state-of-the-art homogeneous and multi-relational graph networks. We demonstrate that our model not only leverages the power of Euclidean networks such as interpretability and efficient execution of various model components, but also outperforms both Euclidean and hyperbolic counterparts on various benchmarks. Our code is made publicly available at <https://github.com/oom-debugger/ijcai23>.

1 Introduction

Graph data structures are ubiquitous. There have been several advancements in graph processing techniques across several domains such as citation networks [Sen *et al.*, 2008], medicine [Anderson and May, 1992], and e-commerce [Choudhary *et al.*, 2022]. Recently, non-Euclidean geometries such as hyperbolic spaces have shown significant potential in representation learning and graph prediction [Chami *et al.*, 2019; Choudhary *et al.*, 2021]. Due to their exponential growth in volume with respect to radius [Krioukov *et al.*, 2010], hyperbolic spaces are able to embed hierarchical structures with low distortion, i.e., an increase in the number of nodes in a tree with increasing depth is analogous to moving outwards from the origin in a Poincaré ball (since both grow exponentially). This similarity enables the hyperbolic space to project the child nodes exponentially further away from the origin compared to their parents (as shown in Figure

1.a) which captures hierarchy in the embedding space. There are certain fundamental questions about hyperbolic models which are yet to be studied. For example, hyperbolic models operate on completely new manifolds with their own gyrovector space [Ungar, 2009] (to be differentiated from the Euclidean vector space). Because they operate in a different manifold, techniques such as dropout or L1/2 regularization do not guarantee similar behavior. Moreover, while existing hyperbolic operations [Ganea *et al.*, 2018] provide fair support for basic sequential neural networks, a correct translation of more complex Euclidean architectures (such as multi-headed attention networks [Vaswani *et al.*, 2017]) is non-trivial and counter-intuitive, due to the special properties of Riemannian manifold [Shimizu *et al.*, 2021]. Finally, hyperbolic operators are computationally expensive i.e., the number of complex mathematical operations for each primitive operator limits their scalability compared to the Euclidean graph neural networks.

Traditionally, hyperbolic models use a mixture of hyperbolic geodesics, gyro-vector space mathematics (e.g. Poincaré disc model combined with Möbius operations), and tangent space approximations at various points. Instead of switching between multiple frameworks with potentially incongruent operations, in this work, we let the Poincaré disk model be our search space and propose to apply all approximations in place on the Poincaré disk (i.e., to apply all tangent space approximations on the disk as if the disk is a tangent space derived from the origin). This enables us to replace non-scalable gyro-vector/Möbius operations with a Euclidean approximation, and then simplify the whole hyperbolic model as a Euclidean model cascaded with a hyperbolic normalization function. In our approach, we replace all Möbius operations with Euclidean operations, yet we still work in the Riemannian manifold (by using our proposed hyperbolic normalization layer along with using Riemannian optimizer), thus, we call it **Pseudo-Poincaré** framework (figure 1.b).

With our formulations, the trainable parameters lie in the Euclidean space, hence we can re-use the architectures that already exist for Euclidean solution space. This leads to the use of inexpensive operators. It also enables the use of existing well-optimized Euclidean models along with their hyperparameter settings tuned for specific tasks. Having the aforementioned two capabilities, our framework brings the best of two worlds together. For further evidence, we have ap-

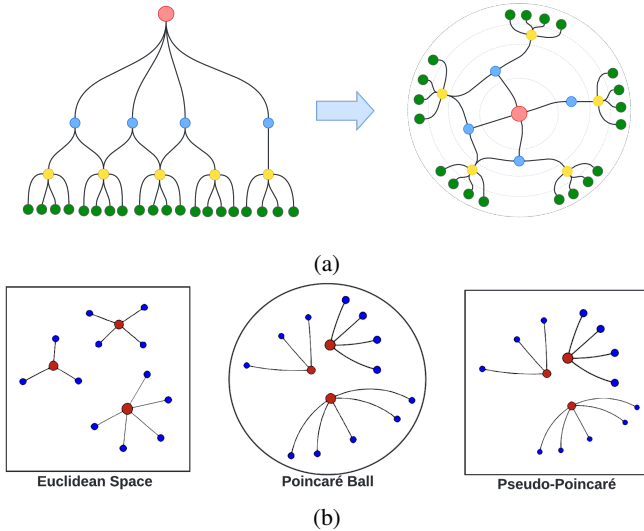


Figure 1: (a) Mapping hierarchical data onto a Poincaré ball. Starting with the root as origin (red), the children are continuously embedded with exponentially increasing distances. (b) Aggregation of vectors in Euclidean, Poincaré Ball, and pseudo-Poincaré space (hyperbolic vectors in Euclidean space). Red points are the aggregation of blue points. Pseudo-Poincaré paradigm reformulates hyperbolic operations to capture hierarchy in Euclidean space.

plied our formulation to construct new pseudo-Poincaré variants of *GCN* [Kipf and Welling, 2017], *GAT* [Veličković *et al.*, 2018], and multi-relational graph embedding model *MuR* [Balažević *et al.*, 2019], *RGCN* [Schlichtkrull *et al.*, 2018] and *GCNII* [Chen *et al.*, 2020] (we call our variants as *NGCN*, *NGAT*, *NMuR*, *NRGCN*, and *NGCNII*, respectively). We demonstrate that the reformulated variants outperform several state-of-the-art graph networks on standard graph tasks. Furthermore, our experiments indicate that our pseudo-Poincaré variants benefit from using regularization methods used in Euclidean counterparts (unlike the traditional hyperbolic counterparts). We also show the execution speed of our proposed model to be comparable to that of the Euclidean counterparts and hence provide insights for building deeper hyperbolic (pseudo-Poincaré) models.

2 Related Work

Research into graph representation learning can be broadly classified into two categories based on the nature of the underlying graph dataset: (i) Homogeneous graphs - where the edges connect the nodes but do not have any underlying information and (ii) Heterogeneous or multi-relational graphs - where the edges contain information regarding the type of connection or a complex relation definition. Early research in this area relied on capturing information from the adjacency matrix through factorization and random walks. In matrix factorization-based approaches [Cao *et al.*, 2015], the adjacency matrix A is factorized into low-dimensional dense matrices L such that $\|L^T L - A\|$ is minimized. In random walk-based approaches [Grover and Leskovec, 2016; Narayanan *et al.*, 2017], the nodes’ information is aggre-

gated through message passing over its neighbors through random or metapath traversal [Fu *et al.*, 2020]. More recently, the focus has shifted towards neighborhood aggregation through neural networks, specifically, Graph Neural Networks (GNNs) [Scarselli *et al.*, 2008]. In this line of work, several architectures such as GraphSage [Hamilton *et al.*, 2017], GCN [Kipf and Welling, 2017], and GAT [Veličković *et al.*, 2018] have utilized popular deep learning frameworks to aggregate information from the nodes’ neighborhood. Concurrently multi-relational graph neural networks have been developed focusing on representation learning in knowledge graphs in which the nodes/entities can have edges/relations of different types. TransE [Bordes *et al.*, 2013], DistMult [Yang *et al.*, 2015], RotatE [Sun *et al.*, 2019], MuRE [Balažević *et al.*, 2019], RGCN [Schlichtkrull *et al.*, 2018] are examples of multi-relational GNNs.

3 Hyperbolic Networks

Manifold hypothesis suggests that high dimensional data tends to lie in the vicinity of a low dimensional manifold [Cayton, 2005][Fefferman *et al.*, 2016]. For such data, the model in fact learns the manifold to better learn the relation between the data points. In graph datasets, hierarchical structures are common, which tend to better align in hyperbolic manifolds. Using the aforementioned concept, Ganea, *et al.* [Ganea *et al.*, 2018] proposed hyperbolic neural networks. Such a network operates in hyperbolic manifolds, simplifies the search space by omitting the manifold learning process, and thus, results in more efficient models for graph applications. That work led to several architectures for representation learning in both homogeneous (HGNC [Chami *et al.*, 2019], HAT [Zhang *et al.*, 2021]) and heterogeneous (MuRP [Balažević *et al.*, 2019], HypE [Choudhary *et al.*, 2021]) graph datasets. These architectures primarily utilize the gyrovector space model to formulate the neural network operations.

Hyperbolic space is a Riemannian manifold with constant negative curvature. The coordinates in the hyperbolic space can be represented in several isometric models such as Beltrami-Klein Model \mathbb{K}_c^n and Poincaré Ball \mathbb{B}_c^n . In this paper, we consider the Poincaré Ball model because it is the most widely used one for hyperbolic networks. In a Poincaré ball of curvature c , simple operations such as vector addition and scaling are done using Möbius operation (addition \oplus_c , scalar multiplication \otimes_c). More complex operations such as aggregation, convolution, and attention are done in local tangent spaces which require transformation between Euclidean and hyperbolic space. For an embedding vector $x \in \mathbb{R}^n$ from point v , its corresponding hyperbolic embedding in the Poincaré ball of curvature c , $p \in \mathbb{B}_c^n$ is calculated with the exponential map as:

$$p = \exp_v^c(x) = v \oplus_c \left(\tanh\left(\frac{\lambda_v \|x\|}{2}\right) \frac{x}{\|x\|} \right), \quad (1)$$

where λ is the conformal factor at point v . Conversely, logarithmic map is used to transform a hyperbolic embedding $p \in \mathbb{B}_c^n$ to a Euclidean vector $x \in \mathbb{R}^n$ is formulated as:

$$x = \log_v^c(p) = \frac{2}{\lambda_v} \tanh^{-1}(\| -p \oplus_c v \|) \frac{-p \oplus_c v}{\| -p \oplus_c v \|}. \quad (2)$$

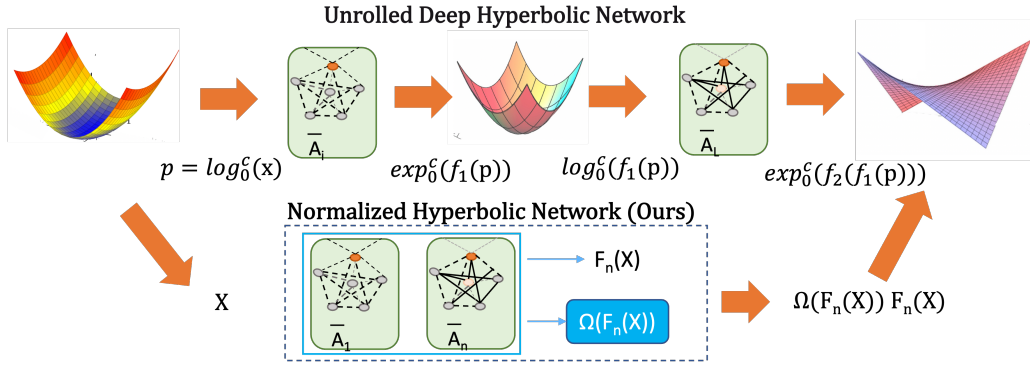


Figure 2: The top row labeled “Unrolled Deep Hyperbolic Network” presents the general idea of stacking deep hyperbolic network with L layers. The input to each layer is passed through a logarithmic map to project onto a Euclidean space, and following the Euclidean layer computation, the output is projected back onto the hyperbolic space. The section “**Hyperbolic Layers**” shows the operator and function chaining technique. Our methodology shown in the lowest layer completely avoids the repeated application of these subspace transformations.

Note that the tangent space approximation relies on the assumption of spatial locality (i.e., small vectors starting from point v). For transporting a local vector from a point in the Hyperbolic manifold to another point, one can use parallel transport [Lee, 2018]. Parallel transport is specifically used in bias addition in Hyperbolic linear layers [Chami *et al.*, 2019]. For a detailed discussion on parallel transport, please refer to [Lee, 2018].

3.1 Hyperbolic Layers

Hyperbolic Feed-forward layer. For the Euclidean function $f : \mathbb{R}^n \rightarrow \mathbb{R}^m$, its equivalent Möbius version $f^{\otimes_c} : \mathbb{B}_c^n \rightarrow \mathbb{B}_c^m$ for the Poincaré ball is defined as $f^{\otimes_c}(p) := \exp_0^c(f(\log_0^c(p)))$. Extending this, the hyperbolic equivalent $h^{\mathbb{B}}(p)$ of the Euclidean linear layer $h^{\mathbb{R}}(x) = Wx$ with weight matrix $W \in \mathbb{R}^{n \times m}$ is formulated as:

$$h^{\mathbb{B}}(p) = \frac{\tanh\left(\frac{|Wp|}{|p|} \tanh^{-1}(\sqrt{c}|p|)\right)}{\sqrt{c}|Wp|} Wp \quad (3)$$

Hyperbolic Convolution. For a hyperbolic graph node representation $p_0 \in \mathbb{B}_c^n$ with neighbors $\{p_i\}_{i=1}^k$. As given in [Chami *et al.*, 2019], the hyperbolic convolution layer $GCN^{\otimes_c} : \mathbb{B}_c^n \rightarrow \mathbb{B}_c^m$ constitutes of a linear transform, followed by neighborhood aggregation¹ which is computed as:

$$h^{\mathbb{B}}(p_i) = W_i \otimes_c p_i \oplus_c b_i$$

$$h_{agg}^{\mathbb{B}}(p_0) = \exp_{p_0}^c\left(\sum_{i=1}^k w_{ij} \log_{p_0}^c(h^{\mathbb{B}}(p_i))\right)$$

$$GCN^{\otimes_c}(p_0) = \exp_0^c\left(\sigma(\log_0^c(h_{agg}^{\mathbb{B}}(p_0)))\right) \quad (4)$$

where $w_{ij} = \text{softmax}_{i=1}^k(MLP(\log_0^c(p_0) || \log_0^c(p_i)))$ is an aggregation weight for neighbors.

Multi-relational Hyperbolic Representation. The multi-relational representations for knowledge graph KG are modeled using a scoring function. For a triplet $(h, r, t) \in KG$,

¹The aggregation occurs in the tangent space as concatenation is not well-defined for hyperbolic space.

where relation $x_r \in \mathbb{R}^n$ connects the head entity $x_h \in \mathbb{R}^n$ to the tail entity $x_t \in \mathbb{R}^n$ and $R \in \mathbb{R}^{n \times n}$ is the diagonal relation matrix, the hyperbolic equivalent $\phi^{\mathbb{B}}(p_h, p_r, p_t)$ of the Euclidean scoring $\phi(x_h, x_r, x_t) = -\|Rx_h - (x_t + x_r)\|^2$ function is computed using the hyperbolic distance $d^{\mathbb{B}}$ as:

$$d^{\mathbb{B}}(p_1, p_2) = \frac{2}{\sqrt{c}} \tanh^{-1}(\sqrt{c} \| -p_1 \oplus_c p_2 \|) \quad (5)$$

4 Pseudo-Poincaré Hyperbolic Networks

While hyperbolic networks show promising results, switching back and forth between Möbius gyro-vector operations and Euclidean tangent approximations (at various points) makes them computationally expensive, limits their extensibility, and makes them less predictable when applying L1/2 regularization and dropout. Furthermore, such back and forth between the manifolds (at variable points) comes with an implicit assumption that the embeddings have spatial locality in all dimensions for the models to be performant. We argue that approximating on tangent space at a variable point does not necessarily increase the approximation accuracy because the spatial locality of the embeddings is not guaranteed in general. Therefore, fixating tangent space to be at the origin can bring both simplicity to the model and performance in general cases. Moreover, only tangent space at origin has a one-to-one mapping with all points on the Poincaré (hyperbolic) half-plane model. This enables us to combine the tangent space approximation with Poincaré half-plane model and apply all approximations in the half-plane. This makes the pseudo-Poincaré networks much easier to understand, develop, and optimize. Fixating the tangent space to the point of origin simplifies the exponential maps (eq. 1) as:

$$p = \exp_0^c(x) = \frac{\tanh(\sqrt{c}|x|)}{\sqrt{c}|x|} x. \quad (6)$$

Conversely, the logarithmic map (eq. 2) is simplified as:

$$x = \log_0^c(p) = \frac{\tanh^{-1}(\sqrt{c}|p|)}{\sqrt{c}|p|} p. \quad (7)$$

Using Eq. (6) and Eq. (7), we reformulate the hyperbolic feed-forward layer. In this section, we only discuss the reformulation for Pseudo-Poincaré Feed-forward Layer. The convolution, attention, and multi-relation layer can be similarly reformulated for the Pseudo-Poincaré paradigm.

Pseudo-Poincaré Feed-forward Layer. We state that cascading hyperbolic feed-forward layers (including linear layers) is equivalent to cascading their Euclidean counterparts and then applying a hyperbolic normalization to the result.

Lemma 1. *For a point in the tangent space at origin $x \in \mathcal{T}_{0_n} \mathbb{B}_c^n$, the exponential map to the hyperbolic space \mathbb{B}_c^n , $\exp_0^c : \mathcal{T}_{0_n} \mathbb{B}_c^n \rightarrow \mathbb{B}_c^n$ $\exp_0^c(x)$, is equivalent to the input scaled by a non-linear scalar function $\omega : \mathbb{R}^n \rightarrow \mathbb{R}^n$, i.e.,*

$$p = \exp_0^c(x) = \omega(x)x; \quad \omega(x) = \frac{\tanh(\sqrt{c}|x|)}{\sqrt{c}|x|} \quad (8)$$

where $\omega(x)$ is the hyperbolic normalization for exponential maps. This follows from equation (1).

Lemma 2. *Let $f^{\otimes c}$ be a single hyperbolic feed-forward layer, and $f^{\otimes c}$ be its euclidean counterpart. Approximating on tangent space at origin for all stages makes the cascade of n hyperbolic feed-forward layers $F_n^{\otimes c} = \{f_i^{\otimes c}\}_{i=1}^n$ to be equivalent to cascading n of their Euclidean counterparts $F_n = \{f_i\}_{i=1}^n$ encapsulated in \log_0^c and \exp_0^c functions, i.e.,*

$$F_n(x) = f_n(f_{n-1}(\dots f_1(x))) \quad (9)$$

$$F_n^{\otimes c}(p) = f_n^{\otimes c}(f_{n-1}^{\otimes c}(\dots f_1^{\otimes c}(p))) = \exp_0^c(F_n(\log_0^c(p)))$$

Proposition Lemma 2 implies that the hyperbolic transformations \exp_0^c and \log_0^c are only needed at the initial and final stages to capture hierarchy in Euclidean networks.

Lemma 3. *For given input features $x = \log_0^c(p) \in \mathbb{R}^n$, a given hyperbolic feed forward layer can be rewritten as $f^{\otimes c}(x) := \omega(f(x))f(x)$.*

From lemmas 2 and 3, we arrive at the following theorem for cascaded hyperbolic layers.

Theorem 4. *Fixating the tangent space to be always at origin, cascaded hyperbolic feed-forward layers $F_n^{\otimes c}$ for Euclidean input $x \in \mathbb{R}^n$ can be reformulated as $F_n^{\otimes c}(x) := \Omega(F_n(x))F_n(x)$, where $\Omega(F_n(x))$ is the hyperbolic normalization for a cascaded hyperbolic feed-forward network. Note that $\omega(\cdot)$ is the exponential transformation factor at the variable level and $\Omega(\cdot)$ is the same at the level of neural networks.*

Hyperbolic Normalization. Theorem 4 allows the cascaded hyperbolic layers to be reformulated in the Euclidean space using a hyperbolic normalization (Ω) function. Our normalization layer resembles the technique proposed in [Salimans and Kingma, 2016] to normalize the weights, which uses the equation; $w = \frac{e^s}{\|v\|}v$, where v is an n -dimensional vector used to learn the direction and s is a trainable parameter. However, unlike weight normalization, hyperbolic normalization happens on the features (and not the weights). Furthermore, hyperbolic normalization uses the \tanh scaling function instead of e^s . However, both are similar in terms of using the feature vector magnitude as the denominator and hence removing the orthogonality of the dimensions.

The ‘‘unrolled deep hyperbolic network’’ (shown in Figure 2) presents the general idea of stacking multiple hyperbolic layers together. The input into each layer is passed through a logarithmic map to project into Euclidean space and its output is projected back onto the hyperbolic space after applying the computations.

Batch-Norm, Layer-Norm vs. Hyperbolic Norm. Batch-Norm tries to reduce the covariant shift and noise [Ioffe and Szegedy, 2015] which means the result of the batch-norm is in Euclidean space. On the other hand, Layer-Norm, and Hyperbolic Norm take vectors to another manifold for better latent space representation [Lei Ba *et al.*, 2016]. Thus, we recommend using Riemannian optimizers when applying our method at least for shallow GNNs (we provided empirical results in the next section). Note that, in order to apply the batch normalization in hyperbolic space, one needs to change its mathematical operations to use Frechet mean [Peng *et al.*, 2021]. The detailed analysis of the effect of hyperbolic batch normalization is outside the scope of this work.

Optimization. The scaling function in Eq. (8) uses the vector norm in the denominator and hence, each dimension depends on the value of other dimensions (i.e., non-orthogonal). Due to this, optimizers that are developed based on the orthogonality assumptions of the dimensions such as ADAM are not expected to produce the most optimal weights. Thus, we choose Riemannian optimizers such as Riemannian ADAM [Becigneul and Ganea, 2019] for our model training. For traditional hyperbolic models, regularization techniques such as L2-regularization do not work as expected since the weights are in hyperbolic space. However, the trainable parameters in our formulation are in the Euclidean space. Hence, we can additionally apply regularization techniques that are applied to Euclidean networks.

Algorithm 1 provides the generalized algorithm for our proposed hyperbolic model.

Algorithm 1: Normalized hyperbolic model.

Input: Input Euclidean model F_L , sample node $x \in \mathbb{R}^n$

Output: Output of Normalized hyperbolic model $F_L^{\otimes c}(x)$;

```

1  $f_0^{\otimes c}(x) = x$ ;
2 for layer  $l : 1 \rightarrow L$  do
3    $x \leftarrow f_{l-1}^{\otimes c}(x)$ ;
4   # Layer  $l$  of the Euclidean model is  $f_l(x)$ 
5    $\omega(f_l(x)) = \frac{\tanh(\sqrt{c}|f_l(x)|)}{\sqrt{c}|f_l(x)|}$ ; using Eq. (8)
    $f_l^{\otimes c}(x) = \omega(f_l(x))f_l(x)$ ; using Lemma 3
6 end
7  $F_n^{\otimes c}(x) = f_L^{\otimes c}(x)$ ;
8 return  $F_L^{\otimes c}(x)$ 

```

4.1 Pseudo-Poincaré Layers

In this section, we dive into the details of a few Pseudo-Poincaré Layers.

Pseudo-Poincaré Graph Convolution. The individual components of the Hyperbolic Graph Convolution, as defined in Eq. (4), can be reformulated as a cascaded hyperbolic feed-forward layer. Thus, we approximate both the aggregation weights and the aggregation function in $\mathcal{T}_0\mathbb{B}_c^n$ as:

$$h_{agg}^{\mathbb{B}}(p_i) = \exp_0^c(\sum_{i=0}^k w_{ij} \log_0^c(h^{\mathbb{B}}(p_i))) \quad (10)$$

With this approximation, we apply Theorem 4 to reformulate reformulate the $GCN^{\otimes c} : \mathbb{B}_c^n \rightarrow \mathbb{B}_c^m$ layers as Normalized GCN $NGCN^{\otimes c} : \mathbb{R}^n \rightarrow \mathbb{R}^m$ over Euclidean inputs $x_0 \in \mathbb{R}^n$ with neighbors $\{x_i\}_{i=1}^k$. This is computed as $NGCN^{\otimes c} := \Omega(GCN(x_0))GCN(x_0)$, where $GCN(x_0)$ is the Euclidean Graph Convolution layer [Kipf and Welling, 2017].

Note that the cascaded feed-forward functions of HGNC [Chami *et al.*, 2019] operate on different tangent spaces, i.e., aggregation weights are calculated at the linear tangent space at origin $\mathcal{T}_0\mathbb{B}_c^n$ whereas the aggregation function as given in Eq. (10) is driven from a linear tangent space at the root node $\mathcal{T}_{p_0}\mathbb{B}_c^n$. An argument to use different tangent spaces for different function is based on the fact that Euclidean approximation is most accurate when the tangent space is close to the true resulting point. For aggregation, using tangent space at p_0 requires an implicit assumption that all aggregated hyperbolic points preserve a form of spatial locality, which implies similarity and not exactly the notion of hierarchy. However, we can still argue that hierarchical structures have a loose form of spatial locality, and hence using $\log_0^c(p)$ will add some noise to the embedding compared to when $\log_{p_0}^c(p)$ is used.

Pseudo-Poincaré Graph Attention Layer. Here, our goal is to project the Euclidean GAT layer onto the hyperbolic space by applying the hyperbolic normalization (e.g., Eq. (8)), then, investigate its approximation in relation to the existing hyperbolic graph attention layers as well as with a true hyperbolic graph attention mechanism.

Hyperbolic attention is formulated as a two-step process (as defined in [Gulcehre *et al.*, 2019]); (1) matching, which computes attention weights, and (2) the aggregation, which takes a weighted average of the values (attention coefficients as weights). Hence, the attention layer can be seen as two cascaded layers, in which the first calculates the attention weights, while the second layer aggregates the weighted vectors. Existing hyperbolic graph attention method [Zhang *et al.*, 2021] $GAT^{\otimes c} : \mathbb{B}_c^n \rightarrow \mathbb{B}_c^m$ views the hyperbolic aggregation as a hyperbolic feed forward layer with a Euclidean weighted average as its function. Similarly $GAT : \mathbb{R}^n \rightarrow \mathbb{R}^m$ [Veličković *et al.*, 2018] also uses weighted-average for the aggregation.

Since we are using Euclidean weighted average over cascaded feed-forward layers, we can apply Theorem 4 to hyperbolic GAT and approximate it in the hyperbolic space with a hyperbolic normalization function and Euclidean GAT as $NGAT^{\otimes c}(x) := \Omega(GAT(x))GAT(x)$.

Pseudo-Poincaré Multi-relational Representation. For Euclidean inputs $x_1, x_2 \in \mathbb{R}^n$ and L1-norm $d^{\mathbb{R}}(x_1, x_2)$, the hyperbolic formulation of the multi-relational hyperbolic distance $d^{\mathbb{B}}(x, y)$, given in Eq. (5) can alternatively be reformulated as $d^{\mathbb{B}}(x_1, x_2) = \omega(x)d^{\mathbb{R}}(x_1, x_2)$. Sim-

ilarly, for Euclidean triplet $(x_h, x_r, x_t) \in \mathbb{R}^n$, the scoring function $\phi^{\mathbb{B}}(p_h, p_r, p_t)$ can also be approximated to $NMuR^{\mathbb{B}}(x_h, x_r, x_t)$ as:

$$\phi^{\mathbb{R}}(x_h, x_r, x_t) = -d^{\mathbb{R}}(Rx_h, x_t + x_r)^2 \quad (11)$$

$$NMuR^{\mathbb{B}}(x_h, x_r, x_t) = \Omega(\phi^{\mathbb{R}}(x_h, x_r, x_t))\phi^{\mathbb{R}}(x_h, x_r, x_t) \quad (12)$$

5 Experimental Results

In this section, we aim to answer following research questions (RQs) through our experiments:

RQ1: How do the pseudo-Poincaré variants compare to their Euclidean and hyperbolic counterparts on node classification and link prediction?

RQ2: How does the pseudo-Poincaré variant, NMuR, compare to its Euclidean and hyperbolic counterparts on reasoning over knowledge graphs?

RQ3: How do pseudo-Poincaré variants react to the choice of optimizers, and what are the effects on their execution time? How does the hyperbolic normalization compare to its counterparts?

RQ4: How does pseudo-Poincaré variant perform when used in deep GNN architectures e.g. GCNII?

RQ5: What is the difference in the representations obtained through hyperbolic and pseudo-Poincaré projections?

5.1 Experimental Setup

For comparison of hyperbolic normalization with other methods, we conduct our experiments on the following tasks: (i) graph prediction (node classification and link prediction) and (ii) reasoning over knowledge graphs, which are described below:

Graph Prediction. Given a graph $\mathcal{G} = (V \times E)$, where $v_i \in \mathbb{R}^n$, $\{v_i\}_{i=1}^{|V|} \in V$ is the set of all nodes and $E \in \{0, 1\}^{|V| \times |V|}$ is the Boolean adjacency matrix, where $|V|$ is the number of nodes in the graph and $e_{ij} = 1$, if link exists between node i and j , and $e_{ij} = 0$, otherwise. Each node $v_i \in V$ is also labeled with a class y_i . In the task of **node classification**, the primary aim is to estimate a predictor model P_θ with parameters θ such that for an input node v_i ; $P_\theta(v_i|E) = y_i$. In the task of **link prediction**, the primary aim is to estimate a predictor model P_θ with parameters θ such that for an input node-pair v_i, v_j and an incomplete adjacency matrix \hat{E} ; $P_\theta(v_i, v_j|\hat{E}) = e_{ij}$, where $e_{ij} \in E$ is an element in the complete adjacency matrix.

Reasoning over Knowledge Graphs. Let us say that a set of triplets constitutes a knowledge graph $\mathcal{KG} = \{(h_i, r_i, t_i)\}_{i=1}^{|\mathcal{KG}|}$, where $h_i \in \mathbb{R}^n$ and $t_i \in \mathbb{R}^n$ are the head and tail entity, respectively connected by a relation $r_i \in \mathbb{R}^n$. In the task of **reasoning** [Balažević *et al.*, 2019], our goal is to learn representations for the entities and relations using a scoring function that minimizes the distance between heads and tails using the relation as a transformation. The scoring function for Euclidean *MuRE*, hyperbolic *MuRP* and pseudo-Poincaré *NMuR* are presented in Eq. (11), and Eq. (12), respectively.

Repr. Space	Datasets Models	Node Classification (Accuracy in %)			Link Prediction (ROC in %)		
		CORA	Pubmed	Citeseer	Cora	Pubmed	Citeseer
Euclidean	GCN	80.1±0.3	78.5±0.3	71.4±0.3	90.2±0.2	92.6±0.2	91.3±0.2
	GAT	82.7±0.2	79.0±0.3	71.6±0.3	89.6±0.2	92.4±0.2	93.6±0.2
Hyperbolic	HGCN	77.9±0.3	78.9±0.3	69.6±0.3	91.4±0.2	95.0±0.1	<u>92.8±0.3</u>
	HGAT	79.6±0.3	79.2±0.3	68.1±0.3	90.8±0.2	93.9±0.2	<u>92.2±0.2</u>
Pseudo-Poincaré	NGCN	82.4±0.2	78.8±0.3	<u>71.9±0.3</u>	<u>91.3±0.2</u>	<u>94.7±0.1</u>	<u>92.8±0.2</u>
	NGAT	83.1±0.2	<u>79.1±0.3</u>	73.8±0.3	90.5±0.2	93.9±0.2	<u>92.8±0.2</u>

Table 1: Performance comparison results between hyperbolic normalization (ours) and the baseline methods on the graph prediction tasks of node classification and link prediction. The columns present the evaluation metrics, which are Accuracy (for node classification) and Area under ROC (ROC) (for link prediction), along with their corresponding 95% confidence intervals. The cells with the best performance are highlighted in bold and the second-best performance are underlined.

5.2 Datasets and Baselines

Datasets. For comparing our model with the baselines, we chose the following standard benchmark datasets;

- **Cora** [Rossi and Ahmed, 2015] contains 2708 publications with paper and author information connected by citation links and classified into 7 classes based on their research areas.
- **Pubmed** [Sen *et al.*, 2008] contains medical publications pertaining to diabetes labeled into 3 classes. The dataset is collected from the Pubmed database.
- **Citeseer** [Sen *et al.*, 2008] contains 3312 annotated scientific publications connected by citation links and classified into 6 classes of research areas.
- **WN18RR** [Dettmers *et al.*, 2018] is a subset of the hierarchical WordNet relational graph that connects words with different types of semantic relations. WN18RR consists of 40,943 entities connected by 11 different semantic relations.
- **FB15k-237** [Bordes *et al.*, 2013] [Toutanova *et al.*, 2015] contains triple relations of the knowledge graph and textual mentions from the Freebase entity pairs, with all simple invertible relations are removed for better comparison. The dataset contains 14,541 entities connected by 237 relations.
- Protein-Protein Interaction (**PPI**) network dataset [Hamilton *et al.*, 2017] contains 12M+ triples with 15 relations (preserving the original ratio of the relations in the dataset, we randomly sampled the dataset, and trained on the sampled subset).

We use Cora, Pubmed, and Citeseer for our experiments on homogeneous graph prediction, i.e., node classification and link prediction. For comparing the multi-relational networks on the task of reasoning, we utilize the FB15k-237 and WN18RR datasets. For a fair comparison of evaluation metrics, we use the same training, validation, and test splits as used in the previous methods, i.e., the splits for Cora, Pubmed, and Citeseer are as given in [Chami *et al.*, 2019] and for FB15k-237 and WN18RR, the splits are in accordance with [Balažević *et al.*, 2019].

Baselines. For comparing the performance of our Pseudo-Poincaré models, we utilize the Euclidean and hyperbolic variants of the architecture as our baselines;

- **Graph Convolution (GCN)** [Kipf and Welling, 2017] aggregates the message of a node’s k-hop neighborhood using a convolution filter to compute the neighbor’s significance to the root.
- **Graph Attention (GAT)** [Veličković *et al.*, 2018] aggregates the messages from the neighborhood using learnable attention weights.
- **Hyperbolic Graph Convolution (HGCN)** [Chami *et al.*, 2019] is a hyperbolic formulation of the GCN network that utilizes the hyperbolic space and consequently, Möbius operations to aggregate hierarchical features from the neighborhood,
- **Hyperbolic Graph Attention (HGAT)** [Yang *et al.*, 2021] is a hyperbolic formulation of the GAT networks to capture hierarchical features in the attention weights.
- **Multi-relational Embeddings (MuRE)** [Balažević *et al.*, 2019] transforms the head entity by a relation matrix and then learns representation by minimizing L1-norm between head and tail entities translated by the relation embedding.
- **Multi-relational Poincaré (MuRP)** [Balažević *et al.*, 2019] is a hyperbolic equivalent of MuRE that transforms the head entity by a relation matrix in the Poincaré ball and then learns representation by minimizing the hyperbolic distance between the head and tail entities translated by the relation embedding.
- **Relational Graph Convolution Network (RGCN)** [Schlichtkrull *et al.*, 2018] is graph convolutional networks applied in heterogeneous graph.
- **Deep Graph Convolutional Networks (GCNII)** [Chen *et al.*, 2020] is an extension of a Graph Convolution Networks with two new techniques, initial residual and identify mapping, to be used in deep GNN settings.

5.3 Implementation Details

Our models are implemented on the Pytorch framework [Paszke *et al.*, 2019] and the baselines are adopted from [Chami *et al.*, 2019] for GAT, GCN, and HGCN, and from [Balažević *et al.*, 2019] for MuRE and MuRP. Due to the unavailability of a public implementation, we use our own implementation of HGAT based on [Yang *et al.*, 2021]. The implementations have been thoroughly tuned with different hyper-parameter settings for the best performance.

Dim Models	WN18RR			FB15K-237			PPI			
	MRR	H@10	H@3	MRR	H@10	H@3	MRR	H@10	H@3	
40	MuRE	40.9±0.3	49.7±0.3	44.5±0.3	29.0±0.3	46.2±0.3	31.9±0.3	2.81±0.3	9.24±0.3	4.11±0.3
	MuRP	42.5±0.3	52.2±0.3	45.9±0.3	29.8±0.3	47.4±0.3	32.8±0.3	5.55±0.3	10.21±0.3	4.43±0.3
	NMuR	43.6±0.3	57.5±0.3	47.4±0.3	31.5±0.3	49.7±0.3	34.7±0.3	8.21±0.3	14.3±0.3	11.7±0.3
200	MuRE	44±0.3	51.3±0.3	45.5±0.3	31.4±0.3	49.5±0.3	34.5±0.3	10.68±0.3	14.55±0.3	11.90±0.3
	MuRP	44.6±0.3	52.4±0.3	46.2±0.3	31.5±0.3	49.8±0.3	34.8±0.3	8.23±0.3	15.09±0.3	9.98±0.3
	NMuR	44.7±0.3	57.9±0.3	48.1±0.3	32.2±0.3	50.6±0.3	35.5±0.3	12.68±0.3	15.07±0.3	13.82±0.3

Table 2: Performance comparison results between Pseudo-Poincaré (ours) and the baseline methods on the task of multi-relational graph reasoning. The columns present the evaluation metrics of Hits@K (H@K) (%) and Mean Reciprocal Rank (MRR) (%) along with their corresponding 95% confidence intervals. The best results are highlighted in bold.

Dataset	AIFB	AM	BGS	MUTAG
RGCN	97.22	89.39	82.76	67.65
NRGCN	97.22	89.9	89.66	73.53
E-RGCN	88.89	90.4	82.76	75.00
NE-RGCN	94.44	90.91	86.21	76.47

Table 3: Node-Classification results for RGCN model on AIFB, AM, BGS, and MUTAG datasets. Note that we used the same implementation and dataset in [Thanapalasingam *et al.*, 2021] to show that our method can be applied incrementally and effectively to the existing code-bases.

Dataset	MPR	Hits@1	Hits3	Hits@10
	FB-Toy			
RGCN	47.0	30.9	55.3	83.2
N-RGCN	51.8	35.2	60.9	86.5
	WN18			
RGCN	65.9	43.2	89.0	93.7
N-RGCN	75.2	59.8	90.2	93.9

Table 4: Link-Prediction results for RGCN model on WN18 and FB-Toy datasets. Note that we used the same implementation and dataset in [Thanapalasingam *et al.*, 2021] to show that our method can be applied incrementally and effectively to the existing code-bases.

For GAT baseline, we used 64 dimensions with 4 and 8 attention heads (we found 4 heads perform better and hence we only present that result in our tables), with dropout rate of 0.6 and L2 regularization of $\lambda = 0.0005$ (for Pubmed and Cora), and $\lambda = 0.001$ (for CiteSeer) to be inline with the hyperparameters reported in [Veličković *et al.*, 2018]. We used same number of dimensions and hyperparameters for our NGAT model. For GCN baseline, [Veličković *et al.*, 2018] used 64 dimensions. we used the same number of dimensions and hyperparameter setting as GAT baseline. It should be noted that, we observed poor performance when we applied regularization techniques (that GAT baseline used) to the hyperbolic models. For HGCN, the original paper used 16 hidden dimension, however, we tried 64, 32, and 16 for the hidden dimensions, we found 64 dimensions produces a better results. For the curvature choice, we used different curvatures for different tasks. For the task of node classification, we used $c = 0.3$ (for Cora), and $c = 1$ (for Pubmed and Citeseer) as they produced the best results, while for the link prediction task, $c = 1.5$ produced the best results. at the end, we empirically found that scaling the output of the hy-

perbolic normalization layer by the factor of 5 produces the best results when $c = 0.3 - 0.5$ (and for $c = 1.5$, we set the scaling factor to 3).

5.4 RQ1: Performance on Graph Prediction

To evaluate the performance of hyperbolic normalization with respect to Euclidean and hyperbolic alternatives, we compare the *NGCN* and *NGAT* models against the baselines on the tasks of node classification and link prediction. We utilize the standard evaluation metrics of accuracy and ROC-AUC for the tasks of node classification and link prediction, respectively (Table 1).

From the results, in all cases (except link-prediction on Citeseer), pseudo-Poincaré variants outperform the Euclidean model. Pseudo-Poincaré variants perform better than their hyperbolic counterparts in node classification, but marginally lower in link-prediction. This is inline with our expectations as embeddings of adjacent points in link-prediction on homogeneous graphs tend to have spatial locality. However, spatial locality is less likely for node-classification (as far away nodes still can belong to the same class). It is also worth noting that Pseudo-Poincaré outperforms Euclidean in all node-classification datasets regardless of the hyperbolicity of the dataset (e.g., Cora has low hyperbolicity [Chami *et al.*, 2019] which were previously suggested as a reason that inferior Hyperbolic networks over Euclidean counterparts). This observation suggests that Pseudo-Poincaré is more general purpose framework (i.e., it is performant in a wider variety of tasks/datasets compared to pure-Hyperbolic model). It should be noted that pseudo-Poincaré variants are consistently at least the second-best performing methods, closely following the top performer which makes it appealing given the low-complexity, and speedup of the model (Table 7).

5.5 RQ2: Multi-relational Reasoning

To compare the performance of hyperbolic normalization against the baselines for multi-relational graphs, we compare the *NMuR* model against *MuRE* and *MuRP* on the task of reasoning. We consider the standard evaluation metrics of Hits@K and Mean Reciprocal Rank (MRR) to compare our methods on the reasoning task. Let us say that the set of results for a head-relation query (h, r) is denoted by $R_{(h,k)}$, then the metrics are computed by $MRR = \frac{1}{n} \sum_{i=1}^n \frac{1}{rank(i)}$ and $Hits@K = \frac{1}{K} \sum_{k=1}^K e_k$, where $e_k = 1$, if $e_k \in R_{(h,r)}$ and 0, otherwise. Here $rank(i)$ is the rank of the i^{th} retrieved

sample in the ground truth. To study the effect of dimensionality, we evaluate the models with two values of the embedding dimensions: $n = 40$ and $n = 200$. The results from our comparison are given in Table 2.

From the results, note that *NMuR* outperforms the hyperbolic model *MuRP*, on an average, by $\approx 5\%$ with 40 dimensions and $\approx 3\%$ with 200 dimensions across various metrics and datasets. This shows that *NMuR* is able to effectively learn better representations at lower number of dimensions. Also, note that the difference in performance by increasing the number of dimensions is $< 1\%$ for most cases, implying that *NMuR* is already able to capture the hierarchical space of the knowledge graphs at lower dimensions. This should limit the memory needed for reasoning without a significant loss in performance.

Applying Pseudo-Poincare to RGCN

In order to further show (1) the effectiveness our method, as well as (2) how easy it is to apply our method to an existing model (i.e. adoptability), we took the pytorch models implemented by [Thanapalasingam *et al.*, 2021], and added our hyperbolic normalization layer as the last layer of the model. We also trained the model using Riemannian Adam. Table 3 shows the comparative results for the Node Classification tasks on AIFB, AM, BGS, and MUTAG datasets (further details about the datasets can be found in [Thanapalasingam *et al.*, 2021]). We used curvature $c = 1.5$, and scaling factor $s = 3$ for N-RGCN and $c = 0.5$, and $s = 5$ for NE-RGCN (except for MUTAG NE-RGCN that we used $c = 1.5$, and $s = 3$). We trained the models 10 time and picked the best checkpoint for both Euclidean and our variant. We observed significant improvements in across all metrics when we applied our Hyperbolic normalization method. The fact the applying our method to the existing models is almost seamless increases the ability to explore/adopt hyperbolic models for variety of tasks/models/applications.

Table 4 shows the results of Link Prediction over WN18 and FB-Toy datasets (we stuck to the same implementation and the datasets to have apple-to-apple comparison). We only trained RGCN (the pytorch implementation they had in 4). We used curvature $c = 1.5$, and scaling factor $s = 3$ for FB-Toy, and $c = 0.5$, and $s = 5$ for WN18 dataset. We trained the model on WN18 for 7k epochs, and on FB-toy for 12K (to replicate the experiments in [Thanapalasingam *et al.*, 2021]).

5.6 RQ3: Model Analysis

Hyperbolic Normalization vs. Layer Normalization. In this experiment, we study the difference between our hyperbolic normalization compared to other existing normalization approaches. For this, we select Layer-norm [Lei Ba *et al.*, 2016] as it is the closest in terms of input/output. Also, in order to study the effect of hyperbolic scaling in our normalization layer, we added constant-norm which is computed as follows: $norm(x) = x/\|x\|$. In order to compare the effect of normalization layers, we did not use any extra hyperparameter tuning and regularization. We set the embedding size to 64 for both GAT and GCN, and used 4 heads for GAT-models. Table 5 shows the comparison of different normalization methods on Cora, Pubmed, and Citeseer datasets, and

Base Model		CR	PM	CS
GCN	Constant	67.9	76.7	68.3
	Layer-Norm	78.3	75.0	63.6
	Hyp-Norm	80.9	78.0	72.1
GAT	Constant	75.3	73.0	61.2
	Layer-Norm	75.6	74.9	65.3
	Hyp-Norm	76.7	76.3	68.6

Table 5: Comparison of normalization methods. (Layer-Norm, Hyperbolic Norm, and Constant magnitude). The columns present results on Cora (CR), Pubmed (PM), and Citeseer (CS) datasets using GAT and GCN models. Note that the provided results are without any hyper-parameter tuning, thus the comparison is only valid column-wise.

Models	Optimizers	Cora	Pubmed	Citeseer
GAT	Adam	82.7±0.2	78.7±0.2	71.6±0.3
	RAdam	78.4±0.3	79.0±0.3	71.1±0.3
HGAT	Adam	76.8±0.3	76.0±0.3	68.1±0.3
	RAdam	79.6±0.3	78.9±0.3	68.1±0.3
NGAT	Adam	78.8±0.3	77.7±0.3	69.7±0.3
	RAdam	83.9±0.2	79.1±0.3	73.8±0.3

Table 6: Performance of NGAT, GAT, and HGAT on node classification with RAdam and Adam optimizers.

confirms the outperformance of hyperbolic normalization. Since Layer-norm keeps the GAT model in the Euclidean space, we used ADAM optimizer. However, since both hyperbolic normalization and constant normalization have $\|x\|$ as their denominator, we used RiemannianAdam.

Optimizer Choice. In this study, we experimentally validate our observations regarding the choice of optimizers. Table 6 shows that NGAT works better when RiemannianAdam is used as an optimizer. This shows that, although the parameters are in the Euclidean space, their gradient updates occur in accordance with hyperbolic gradients. Thus, NGAT leverages the architecture of GAT, but behaves more closely to HGAT when it comes to parameter optimization.

Execution Time Comparison. In this analysis, we demonstrate the impact of hyperbolic normalization in improving the scalability of hyperbolic networks. We study the computational cost to train our model versus the hyperbolic and Euclidean counterparts. We ran all the experiments on Quadro RTX 8000 with 48GB memory, and reported the mean of *epoch/second* for each training experiment for link prediction task in Table 7. Our model NGCN is 3 times faster than the HGCN on average over the entire training, while NGAT is 5 times faster than its own hyperbolic counterpart (HGAT). NGCN and NGAT are 25% and 12% slower compared to their Euclidean counterparts, respectively. We observed the smallest speedup for Pubmed which is due to the large dataset memory footprint. Even in this case, our NGCN model is still more than 2 times faster than HGCN and NGAT is more than 3.5 times faster than HGAT.

5.7 RQ4: Hyperbolic Norm on Deep GNNs

[Li *et al.*, 2018] indicates the traditional GNNs such as GCN and GAT achieve their best performance with 2-layer mod-

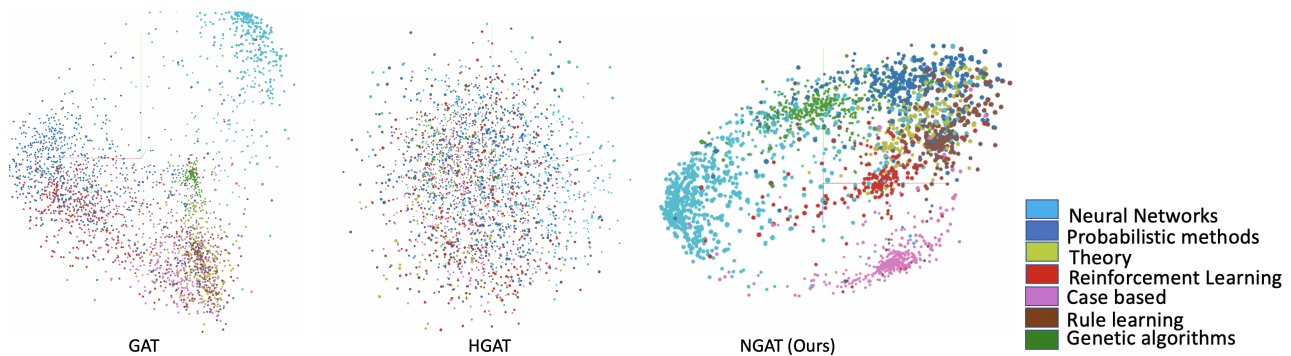


Figure 3: Embedding visualizations of the Cora citation graph for Euclidean (GAT), hyperbolic (HGAT), and our proposed Pseudo-Poincaré (NGAT) methods. NGAT achieves better separation between the node classes than the corresponding Euclidean and hyperbolic counterparts.

Model		CR	PM	CS
Convolution	GCN	0.07	0.13	0.04
	HGCN	0.29	0.33	0.21
	NGCN	0.08	0.14	0.06
Attention	GAT	0.16	0.38	0.09
	HGAT	1.10	1.34	0.81
	NGAT	0.19	0.37	0.12

Table 7: Comparison of execution times. The training epoch times (in seconds - lower is better) for Euclidean, hyperbolic, and Pseudo-Poincaré models.

els. Stacking more layers and adding non-linearity tends to degrade the performance of these models. Such a phenomenon is called over-smoothing. So far, in our experiment, we showed that adding our hyperbolic normalization layer (plus riemannian Adam optimizer) increases the model performance. In order to understand the behavior of our layer on deep GNNs, we experimented on GCNII with 2, 4, 8, 16, 32, and 64 layers. Please note that since our hyperbolic normalization layer contains tanh, adding the normalization layer to all GCNII causes vanishing gradient descent problem. Thus, we only used our hyperbolic normalization layer in the middle of the model to form and encoder-decoder model (in which the encoder creates a hyperbolic latent space, and a normal decoder interprets the latent space). We picked the same Euclidean hyper-parameters as the original GCNII work [Chen *et al.*, 2020] but did grid search on curvature and scale. Table 8 shows the results for Cora, Citeseer, Pubmed node classification tasks. As a general observation, the best pick (across models with different layers) of our normalized N-GCNII is either on par or outperforms the best pick of Euclidean GCNII. However, when we look more granular, we observe our model (N-GCNII), outperform the Euclidean counterpart with bigger margin in the shallow models. As the number of layers increases, the performance gap reduces as well. We believe this is due to the fact that deeper model are better at learning smooth manifolds which is consistent with studies on NLP indicating the latent space of deep models shows a degree of hyperbolicity [Chen *et al.*, 2021]. Moreover, we observed that as the model gets deeper, applying Riemannian Adam is less effective (for models deeper than 8 layers, ADAM performs better even on our models).

	Models	2	4	8	16	32	64
Cora	GCNII	83.1	83.6	84.6	85.6	86.4	86.1
	NGCNII	83.6	84.5	85.4	85.8	86.3	86.1
Citeseer	GCNII	68.7	69.1	71.3	73.4	73	73.2
	NGCNII	69.8	70.2	68.8	73.6	74.1	73.1
Pubmed	GCNII	78.6	78.5	79	80.8	80.2	80.4
	NGCNII	79.4	79.2	80	80.5	80.9	80.5

Table 8: The behavior of hyperbolic normalization on deep GNNs.

5.8 RQ5: Embedding Visualizations

We visually demonstrate that our approach of learning in Euclidean space, indeed preserves the hierarchical characteristics of hyperbolic space. Towards this goal, we present the visualization of node embeddings from the Cora citation graph. We choose Cora, since it is a citation-based graph and does not contain explicit hierarchical (is-a) relations. We contrast the embeddings learned by GAT (a method based on Euclidean space), with HGAT (learning in hyperbolic space) with the proposed NGAT approach. Figure 3 shows that NGAT ensures clearer separation between node classes in comparison to its Euclidean and hyperbolic counterparts.

6 Conclusion

In this paper, we showed that a Euclidean model can be converted to behave as a hyperbolic model by simply (1) connecting it to the hyperbolic normalization layer and (2) using a Riemannian optimizer. From the training perspective, this approach allows the trainable parameters to interact in the Euclidean vector space, consequently enabling the use of Euclidean regularization techniques for the model training. Furthermore, the training of our proposed approach is significantly faster compared to the existing hyperbolic methods. This allows the hyperbolic networks to be more flexible in practice to a wider variety of graph problems. From task perspective, we removed the implicit assumption of having spatial locality of the adjacent nodes (in all dimensions), to be a prerequisite of the hyperbolic model training. This allows the framework to be applied on a wider range of tasks.

References

- [Anderson and May, 1992] Roy M Anderson and Robert M May. *Infectious diseases of humans: dynamics and control*. Oxford university press, 1992.
- [Balažević *et al.*, 2019] Ivana Balažević, Carl Allen, and Timothy Hospedales. Multi-relational poincaré graph embeddings. In *Advances in Neural Information Processing Systems*, 2019.
- [Becigneul and Ganea, 2019] Gary Becigneul and Octavian-Eugen Ganea. Riemannian adaptive optimization methods. In *International Conference on Learning Representations*, 2019.
- [Bordes *et al.*, 2013] Antoine Bordes, Nicolas Usunier, Alberto Garcia-Duran, Jason Weston, and Oksana Yakhnenko. Translating embeddings for modeling multi-relational data. *Advances in neural information processing systems*, 26, 2013.
- [Cao *et al.*, 2015] Shaosheng Cao, Wei Lu, and Qiongkai Xu. Grarep: Learning graph representations with global structural information. In *Proceedings of the 24th ACM international conference on information and knowledge management*, pages 891–900, 2015.
- [Cayton, 2005] Lawrence Cayton. Algorithms for manifold learning. *Univ. of California at San Diego Tech. Rep*, 12(1-17):1, 2005.
- [Chami *et al.*, 2019] Ines Chami, Zhitao Ying, Christopher Ré, and Jure Leskovec. Hyperbolic graph convolutional neural networks. In *Advances in Neural Information Processing Systems*, pages 4869–4880, 2019.
- [Chen *et al.*, 2020] Ming Chen, Zhewei Wei, Zengfeng Huang, Bolin Ding, and Yaliang Li. Simple and deep graph convolutional networks. In Hal Daumé III and Aarti Singh, editors, *Proceedings of the 37th International Conference on Machine Learning*, volume 119 of *Proceedings of Machine Learning Research*, pages 1725–1735. PMLR, 13–18 Jul 2020.
- [Chen *et al.*, 2021] Boli Chen, Yao Fu, Guangwei Xu, Pengjun Xie, Chuanqi Tan, Mosha Chen, and Liping Jing. Probing bert in hyperbolic spaces. *arXiv preprint arXiv:2104.03869*, 2021.
- [Choudhary *et al.*, 2021] Nurendra Choudhary, Nikhil Rao, Sumeet Katariya, Karthik Subbian, and Chandan K. Reddy. Self-supervised hyperboloid representations from logical queries over knowledge graphs. In *Proceedings of the Web Conference 2021*, WWW '21, page 1373–1384, 2021.
- [Choudhary *et al.*, 2022] Nurendra Choudhary, Nikhil Rao, Sumeet Katariya, Karthik Subbian, and Chandan K. Reddy. Anthem: Attentive hyperbolic entity model for product search. In *Proceedings of the Fifteenth ACM International Conference on Web Search and Data Mining*, WSDM '22, page 161–171, New York, NY, USA, 2022. Association for Computing Machinery.
- [Dettmers *et al.*, 2018] Tim Dettmers, Pasquale Minervini, Pontus Stenetorp, and Sebastian Riedel. Convolutional 2d knowledge graph embeddings. In *Proceedings of the AAAI conference on artificial intelligence*, volume 32, 2018.
- [Fefferman *et al.*, 2016] Charles Fefferman, Sanjoy Mitter, and Hariharan Narayanan. Testing the manifold hypothesis. *Journal of the American Mathematical Society*, 29(4):983–1049, 2016.
- [Fu *et al.*, 2020] Xinyu Fu, Jiani Zhang, Ziqiao Meng, and Irwin King. Magnn: Metapath aggregated graph neural network for heterogeneous graph embedding. In *WWW*, 2020.
- [Ganea *et al.*, 2018] Octavian Ganea, Gary Bécigneul, and Thomas Hofmann. Hyperbolic neural networks. In *Advances in neural information processing systems*, pages 5345–5355, 2018.
- [Grover and Leskovec, 2016] Aditya Grover and Jure Leskovec. node2vec: Scalable feature learning for networks. In *Proceedings of the 22nd ACM SIGKDD international conference on Knowledge discovery and data mining*, pages 855–864, 2016.
- [Gulcehre *et al.*, 2019] Caglar Gulcehre, Misha Denil, Mateusz Malinowski, Ali Razavi, Razvan Pascanu, Karl Moritz Hermann, Peter Battaglia, Victor Bapst, David Raposo, Adam Santoro, and Nando de Freitas. Hyperbolic attention networks. In *International Conference on Learning Representations*, 2019.
- [Hamilton *et al.*, 2017] William L. Hamilton, Rex Ying, and Jure Leskovec. Inductive representation learning on large graphs. In *NIPS'17*, 2017.
- [Ioffe and Szegedy, 2015] Sergey Ioffe and Christian Szegedy. Batch normalization: Accelerating deep network training by reducing internal covariate shift. In *International conference on machine learning*, pages 448–456. PMLR, 2015.
- [Kipf and Welling, 2017] Thomas N. Kipf and Max Welling. Semi-supervised classification with graph convolutional networks. In *5th International Conference on Learning Representations, ICLR 2017, Toulon, France, April 24-26, 2017, Conference Track Proceedings*. OpenReview.net, 2017.
- [Krioukov *et al.*, 2010] Dmitri Krioukov, Fragkiskos Papadopoulos, Maksim Kitsak, Amin Vahdat, and Marián Boguná. Hyperbolic geometry of complex networks. *Physical Review E*, 82(3):036106, 2010.
- [Lee, 2018] John M Lee. *Introduction to Riemannian manifolds*, volume 176. Springer, 2018.
- [Lei Ba *et al.*, 2016] Jimmy Lei Ba, Jamie Ryan Kiros, and Geoffrey E. Hinton. Layer Normalization. *arXiv e-prints*, page arXiv:1607.06450, July 2016.
- [Li *et al.*, 2018] Qimai Li, Zhichao Han, and Xiao-Ming Wu. Deeper insights into graph convolutional networks for semi-supervised learning. In *Thirty-Second AAAI conference on artificial intelligence*, 2018.
- [Narayanan *et al.*, 2017] Annamalai Narayanan, Mahinthan Chandramohan, Rajasekar Venkatesan, Lihui Chen, Yang

- Liu, and Shantanu Jaiswal. graph2vec: Learning distributed representations of graphs. *arXiv preprint arXiv:1707.05005*, 2017.
- [Paszke *et al.*, 2019] Adam Paszke, Sam Gross, Francisco Massa, Adam Lerer, James Bradbury, Gregory Chanan, Trevor Killeen, Zeming Lin, Natalia Gimelshein, Luca Antiga, et al. Pytorch: An imperative style, high-performance deep learning library. *Advances in neural information processing systems*, 32:8026–8037, 2019.
- [Peng *et al.*, 2021] Wei Peng, Tuomas Varanka, Abdelrahman Mostafa, Henglin Shi, and Guoying Zhao. Hyperbolic deep neural networks: A survey. *arXiv preprint arXiv:2101.04562*, 2021.
- [Rossi and Ahmed, 2015] Ryan A. Rossi and Nesreen K. Ahmed. The network data repository with interactive graph analytics and visualization. In *AAAI*, 2015.
- [Salimans and Kingma, 2016] Tim Salimans and Diederik P. Kingma. Weight normalization: A simple reparameterization to accelerate training of deep neural networks. In *Proceedings of the 30th International Conference on Neural Information Processing Systems, NIPS’16*, page 901–909, Red Hook, NY, USA, 2016. Curran Associates Inc.
- [Scarselli *et al.*, 2008] Franco Scarselli, Marco Gori, Ah Chung Tsoi, Markus Hagenbuchner, and Gabriele Monfardini. The graph neural network model. *IEEE transactions on neural networks*, 20(1):61–80, 2008.
- [Schlichtkrull *et al.*, 2018] Michael Schlichtkrull, Thomas N Kipf, Peter Bloem, Rianne van den Berg, Ivan Titov, and Max Welling. Modeling relational data with graph convolutional networks. In *European semantic web conference*, pages 593–607. Springer, 2018.
- [Sen *et al.*, 2008] Prithviraj Sen, Galileo Mark Namata, Mustafa Bilgic, Lise Getoor, Brian Gallagher, and Tina Eliassi-Rad. Collective classification in network data. *AI Magazine*, 29(3):93–106, 2008.
- [Shimizu *et al.*, 2021] Ryohei Shimizu, YUSUKE Mukuta, and Tatsuya Harada. Hyperbolic neural networks++. In *International Conference on Learning Representations*, 2021.
- [Sun *et al.*, 2019] Zhiqing Sun, Zhi-Hong Deng, Jian-Yun Nie, and Jian Tang. Rotate: Knowledge graph embedding by relational rotation in complex space. In *International Conference on Learning Representations*, 2019.
- [Thanapalasingam *et al.*, 2021] Thiviyan Thanapalasingam, Lucas van Berkel, Peter Bloem, and Paul Groth. Relational graph convolutional networks: A closer look, 2021. arXiv:2107.10015.
- [Toutanova *et al.*, 2015] Kristina Toutanova, Danqi Chen, Patrick Pantel, Hoifung Poon, Pallavi Choudhury, and Michael Gamon. Representing text for joint embedding of text and knowledge bases. In *Proceedings of the 2015 conference on empirical methods in natural language processing*, pages 1499–1509, 2015.
- [Ungar, 2009] Abraham Albert Ungar. *A Gyrovector Space Approach to Hyperbolic Geometry*. Synthesis Lectures on Mathematics & Statistics. Morgan & Claypool Publishers, 2009.
- [Vaswani *et al.*, 2017] Ashish Vaswani, Noam Shazeer, Niki Parmar, Jakob Uszkoreit, Llion Jones, Aidan N Gomez, Łukasz Kaiser, and Illia Polosukhin. Attention is all you need. In *Advances in neural information processing systems*, pages 5998–6008, 2017.
- [Veličković *et al.*, 2018] Petar Veličković, Guillem Cucurull, Arantxa Casanova, Adriana Romero, Pietro Liò, and Yoshua Bengio. Graph Attention Networks. *International Conference on Learning Representations*, 2018. accepted as poster.
- [Yang *et al.*, 2015] Bishan Yang, Wen-tau Yih, Xiaodong He, Jianfeng Gao, and Li Deng. Embedding entities and relations for learning and inference in knowledge bases. In *3rd International Conference on Learning Representations, ICLR*, 2015.
- [Yang *et al.*, 2021] Tianchi Yang, Linmei Hu, Chuan Shi, Houye Ji, Xiaoli Li, and Liqiang Nie. Hgat: Heterogeneous graph attention networks for semi-supervised short text classification. *ACM Transactions on Information Systems (TOIS)*, 39(3):1–29, 2021.
- [Zhang *et al.*, 2021] Yiding Zhang, Xiao Wang, Chuan Shi, Xunqiang Jiang, and Yanfang Fanny Ye. Hyperbolic graph attention network. *IEEE Transactions on Big Data*, pages 1–1, 2021.

Appendices

A Proof of Lemma 2

Given $x \in \mathbb{R}^n$ is a Euclidean equivalent of Poincaré ball’s point $p \in \mathbb{B}_c^n$ in the tangent space at origin $T_{0^n} \mathbb{B}_c^n$. The relation between x and p , as defined by [Ganea *et al.*, 2018] as;

$$p = \exp_0^c(x) = \tanh(\sqrt{c}\|x\|) \frac{x}{\sqrt{c}\|x\|},$$

$$x = \log_0^c(p) = \tanh^{-1}(\sqrt{c}\|p\|) \frac{p}{\sqrt{c}\|p\|},$$

Simplifying with $\omega(x) = \frac{\tanh(\sqrt{c}\|x\|)}{\sqrt{c}\|x\|}$ and $\omega_{\mathbb{B}_c^n}(p) = \frac{\tanh^{-1}(\sqrt{c}\|p\|)}{\sqrt{c}\|p\|}$ results in:

$$p = \omega(x)x \text{ and } x = \omega_{\mathbb{B}_c^n}(p)p \quad (13)$$

B Proof of Lemma 3 and Theorem 1

Let us first look at the case of $n = 1$, i.e., a single hyperbolic feed-forward layer. This is defined by [Ganea *et al.*, 2018] as;

$$F_1^{\otimes c}(p) = f_1^{\otimes c}(p) = \exp_0^c(f_1(\log_0^c(p))) \quad (14)$$

Reformulating this with Lemma 1,

$$F_1^{\otimes c}(p) = \omega(f_1(\log_0^c(p)))f_1(\log_0^c(p));$$

Substituting, $x = \log_0^c(p)$; $F_1^{\otimes c}(p) = \omega(f_1(x))f_1(x)$; (15)

Extending this to $n = 2$,

$$F_2^{\otimes c}(p) = f_2^{\otimes c}(f_1^{\otimes c}(x)) = f_2^{\otimes c}(\omega(f_1(x))f_1(x))$$

Given that $f_1(x)$ is a linear function;

$$f(ax) = af(x); \quad (16)$$

$$F_2^{\otimes c}(p) = \omega(f_1(x))f_2^{\otimes c}(f_1(x));$$

$$F_2^{\otimes c}(p) = \omega(f_1(x))\omega(f_2(x))f_2(f_1(x));$$

$$F_2^{\otimes c}(p) = \omega(f_2(x))\omega(f_1(x))F_2(x);$$

Substituting;

$$\Omega(F_2(x)) = \omega(f_1(x))\omega(f_2(x)); \quad (17)$$

$$F_2^{\otimes c}(p) = \Omega(F_2(x))F_2(x); \quad (18)$$

Extending the above formulation to arbitrary n ,

$$F_n^{\otimes c}(p) = \omega(f_n(x))\dots\omega(f_2(x))\omega(f_1(x))F_n(x);$$

Reformulating this with Lemma 1, we get the conclusion of Lemma 2;

$$F_n^{\otimes c}(p) = \exp_0^c(F_n(\log_0^c(p))); \quad (19)$$

Substituting;

$$\Omega(F_n(x)) = \omega(f_n(x))\dots\omega(f_2(x))\omega(f_1(x)); \quad (20)$$

We get the conclusion of Theorem 1;

$$F_n^{\otimes c}(p) = \Omega(F_n(x))F_n(x);$$